SPE 69394

# Scaling Up of Laboratory Relative Permeability Curves. An Advantageous Approach Based on Realistic Average Water Saturations

**M. A. Crotti**, SPE, Inlab S.A. and **R. H. Cobeñas**, SPE, Chevron San Jorge

## Abstract

Accordingly with Welge formulation, to obtain relative permeability curves at laboratory, all calculations are made on a selected point of the sample. Usually this point is located at the outlet face of the sample, where production rates are directly measured. As a result, relative permeability curves are reported as function of point saturations and not as function of average saturations. Laboratory curves are then adapted to reproduce reservoir behavior, usually through the derivation of pseudo functions. With usual methodologies, this pseudo curves are also expressed as function of point saturations and introduced in numerical simulators. In spite of this procedure, numerical simulators perform their calculations using the average water saturation at every grid block. Although point and average saturations are expected to be the same at infinitely small grid size, this is not the case with coarse areal simulation grids.

In this paper, water-cut as a function of produced oil is analyzed for a linear case. Several cases are developed using relative permeability curves defined as function of point saturations for different grid sizes, and as a function of average water saturation. It is shown that only curves with average values give reliable data.

As a result of this work, an advantageous methodology to transform laboratory measured curves into those consistent with numerical simulation approach is presented. It is also shown that the use of rock relative permeability curves, previously adapted to the particular geometry of the system under study, drastically reduces the number of grid blocks required and overcomes numerical dispersion.

## Introduction

Relative permeability curves are of extreme importance during reservoir evaluations due to their ability of predicting fluid production during reservoir exploitation. They establish, for any particular phase, a functional dependence between phase saturation and the rock ability to produce it.

These curves are determined in special core analysis laboratories through a sequence of measurements and calculations that can be summarized as follows:

1. Measurement of global properties and parameters. These measurements includes geometrical parameters (length, area and poral volume of the sample), fluids properties (viscosities), displacement conditions (pressure difference or flow rate) and extreme point behavior.

2. Displacement test. During the test, produced fluid volumes are recorded as a function of time. It should be mentioned that standard test conditions greatly diminish the influence of gravity and capillary forces. So, results of the test are assumed to be only function of viscous forces.

3. Computation of relative permeability curves. The curves are calculated using some adaptations of frontal advance theory.

As an example of steps 1 and 2 of the previous sequence, Jones y Roszelle[1] experimental data set is shown in **Tables 1** and **2**, and in **Fig. 1**. This particular dataset was selected for the present study due to the fact that any interested reader can easily have access to the detailed sequence of measurements, but it should be pointed out that any laboratory set of data could have been used to fulfill this study's objectives.

**Computation of Relative Permeability Curves**
Before getting into the details of the usual computation of relative permeability curves during explicit calculation (JBN[2] or JR[1] methods), it is convenient to show that based on **Tables 1** and **2** data, and through easy mathematics, it can be computed:

1. ***The average water saturation of the sample***. As long as the oil production is recorded at every time during the test, it is possibly to determine the average water saturation of the sample by performing a material balance.

2. ***The fluid production rates***. By fitting the measured fluid volumes produced against time ($V_o$ vs. $t$ and $V_t$ vs. $t$) the rates of the producing fluids can be obtained on a time basis. Physically, these rates correspond to the ones at end or outer face of the plug.

In this way, Darcy formulation for linear systems can be applied using the available data and obtain relative permeabilities values with the following equations:

$$kr_o = \frac{q_o \cdot A}{k \cdot \mu_o} \cdot \left( \frac{\Delta P}{L} \right) \dots\dots\dots\dots\dots\dots\dots\dots\dots\dots\dots\dots(1)$$

$$kr_w = \frac{q_w \cdot A}{k \cdot \mu_w} \cdot \left( \frac{\Delta P}{L} \right) \dots\dots\dots\dots\dots\dots\dots\dots\dots\dots\dots\dots(2)$$

where $\Delta P$ is assumed to be the same owing to negligible capillary forces

The resulting curves and the average water saturation of the sample are presented in **Table 3**. On a first glance, the data set used in Darcy´s formulation (eqs. 1 and 2) is not consistent because it involves:

- Average values for fluid saturations and pressure gradients.
- Point values for the rate of both phases corresponding to the end face of the porous media.

For this reason, in the explicit solution of frontal advance theory (JBN[2] or JR[1] methods), all the computations are performed using point values. As a result, the calculus is more complex because it involves curve fitting, numerical first and second derivative computations and regardless of potential heterogeneities in the porous media, the results are assumed to become from a homogeneous sample.

Conceptually, frontal advance theory developments[2-4] allow solving the system giving pressure gradients and fluid saturations at the production face of the sample. In this way, the use of Darcy law as presented above, leads to a set of relative permeability values as a function of point saturation (saturation at the outer face of the porous sample). It is then apparent that relative permeability curves computed using frontal advance theory gives consistent results. These values are presented in **Table 4** using the regular way in which laboratories generate relative permeability reports.

Two different ways of performing relative permeabilities curves calculation have been just analyzed. A first, simplified methodology based on direct application of Darcy law and the regular explicit adaptation of frontal advance theory. **Figs. 2** to **4** show the differences between the curves obtained with both methods.

The scope of this paper is devoted to compare the classical, homogeneous and, at first glance, consistent methodology, with the simplified and apparently non-consistent calculation previously described. The results impact on the regular use of relative permeabilities and the scaling up.

## Application of Relative Permeability Curves

The relative permeability curves are used in frontal advance computations, material balance and numerical reservoir simulations.

For the case of frontal advance, the relative permeability curves as reported by laboratories are of direct usage because they are computed, on purpose, to represent this physical answer of the tested porous media.

In a material balance, the situation is very different. In fact, it is expected that relative permeability curves would adequately relate average saturation within the reservoir and total fluid production through the wells. This is the same "non-consistent" relationship obtained with basic laboratory data and the simplified methodology previously presented. Therefore it can be concluded that "consistency" in the way it was previously defined (all data referred to the outer face of the sample) is not a warranty of direct usage of the results.

As a consequence, numerical simulation was studied in more detail. On one side, it is generally assumed in an implicit way, that with a huge number of gridcells of tiny size, relative permeability curves are of direct application and any modification of its shape it is only related to representativity, scale factors or predominant flux forces issues. On the other hand, as the cells although small are of finite volume, a function that relates average fluid saturations and block side production should be required, like in the material balance case.

In this work the results of a series on 1D numerical simulation are analyzed in order to solve this puzzle. The cases analyzed include different number of gridcells and different computation methodologies of relative permeability curves. The obtained results are contrasted with the experimental values presented by Jones y Roszelle[1] in their work.

## Results

### Number of Gridcells

In a first stage, a linear 1D numerical simulation using the laboratory relative permeability curves (point water saturation at the end face of the sample) with only 3 gridcells between the injector and producer was performed.

In the Jones and Roszelle methodology[1], the experimental conditions are set in a way that capillary forces result negligible and the production curve is assumed to be only product of viscous forces. In the numerical simulation, using a capillary curve with null values above $Sw_{irr}$ honored this condition.

The evolution of the produced water cut against adimensional cumulative production ($Np/N$) is presented in **Fig. 5**. In this figure, the experimental results obtained by Jones and Roszelle are also plotted for comparison. According with the usual interpretation the difference between the experimental and simulation results was attributed to the numerical dispersion generated by the low number of gridcells

used. So, the number of gridcells was increased in order to obtain a better match.

**Fig. 6** shows the improvements of simulation results as the gridcells number increases, although it is clearly seen that even using 6,480 gridcells in a linear simulation, an adequate description of the physical system could not be obtained.

### L. Dake Approach
It should also be mentioned that numerical simulators generate, through interpolation techniques, relative permeability values between $Sw_{irr}$ (35.5% in this particular case) and the water breakthrough saturation value (51.1% for this case). This is *ad-hoc* performed to allow the average gridcell water saturation to take values below water breakthrough. According to the frontal advance theory, the relative permeability curves are not defined in the mentioned range and that is why in Jones and Roszelle study, the lines in that range appear with dots.

In the case under study, **Fig. 1** shows that during the first 7 cm$^3$ of oil production, although there is no water production, the average water saturation of the sample continuously increases. However, the point water saturation (at the end face of the sample) remains at $Sw_{irr}$ (35.5 %) until it instantaneously grows to the water breakthrough value (51.1 %). This issue was previously discussed by L. Dake[5] who proposed an empirical partial solution to the numerical dispersion problem by generating step functions in the saturation range not defined by the frontal advance theory of Buckley and Leverett[2].

The curve type proposed by Dake, and the result of its implementation in a linear numerical simulation with only 3 gridcells is presented as **Figs. 7** and **8**. In **Fig. 8** an important improvement regarding the regular use of point relative permeability curves is observed although the match remains still unsatisfactory. In this case, the numerical dispersion is avoided in a wide range of water saturations, but once the water breakthrough is reached the results describe the same misfit as shown in **Fig. 5**.

**Fig. 9** shows the simulation results of applying Dake´s methodology on the relative permeability curve constructed with average water saturation values. For this case water breakthrough is too much delayed.

### Proposed Solution
By comparing **Figs. 8** and **9** it can be inferred that an adequate combination of both relative permeability curves (average and point saturation) adapted with Dake´s correction could better describe the actual physics of the problem. Several schemes were tested in order to have a good match using just 3 gridcells models. The best match was obtained by using an individual relative permeability curve for each of the gridcells.

**Fig. 10** shows a sketch of the linear porous media, with the mixing coefficients of the relative permeability curves (point and average based) used for each of the 3 cells. The results of the numerical simulation using these adapted curves are presented in **Fig. 11** where an excelent agreement between experimental and calculated response can be observed.

### Conceptual Basis for the Solution
Permeability is generally defined as the "ability of a porous media to conduct fluids". In one-phase measurements it is generally calculated through the rate of fluid production or injection, assuming that injection, conduction and production rates are identical. In multiphase flow, the relative permeability concept is included as a correction factor in Darcy´s law as a way to adapt the original equation. But while during the flow of an incompressible phase, the terms "inject", "conduct" and "produce" can be interchanged, this is not the case when more than one-phase flows through the porous media.

For this reason, it can be said that the presently developed solution is based on an efficient definition and usage of the terms "injection", "conduction" and "production" of fluids and the significant difference between "average water saturation" and "point water saturation" in multiphase systems. The goodness of the observed fit is a direct consequence of including the adequate variables during the upscaling step.

**Figs. 12** and **13** sketches the relationship between average water saturation and point water saturation in a linear system of 3 gridcells.

Due to the independence of Welge equations with system length, the first cell in a system of many gridcells keeps the same relationship among its variables as the one that exists in a one-cell system. This is a similar case as the material balance where the relative permeability curves vs. average water saturation always describes the relationship between water saturation of the cell (average) and its point production.

On the other hand, as it is shown in **Fig 13**, when the number of gridcells between the injection and production site increases, the average gridcell water saturation and the point saturation at the production location become nearly similar. So the point saturation curve computed using the frontal advance theory, adequately describes the last gridcell of a multi-cell system.

Hence, it could be assumed that an adequate linear combination of the two types of relative permeability curves could reasonably represent the behavior of the intermediate gridcells. The selected coefficients used in the proposed solution are presented in **Fig 10** and the quality of the final match shows the accuracy of the methodology. This type of mixing rule is easily programmable for automatic computation in numerical simulators.

It must be noted that while the step function proposed by L. Dake was used in this work (Fig. 7) the shape of the correct "step" function betwen Swirr and Sw at Breakthrough is affected by actual relative permeability functions and mobility ratio. Nevertheless, as shown in the present case, the L. Dake simplified step function act as a fairly good first approach to the exact solution

## Considerations

A global consequence of the study here presented is that no matter which is the selected way to construct the relative permeability curve for a given set of fluids and porous media, a different curve is needed for cells located at different position in the numerical simulator. This is not an avoidable characteristic, but a physical need. Fortunately, as shown in this paper, a simplified way to construct the curves for every cell exists.

The implicit calculation for laboratory relative permeability curves does not overcome the problem here discussed. The "only" computed solution with this methodology depends on the number of cells in the simulator which differs from the curve needed when using scarce number of cells typical of practical simulation cases.

The usually proposed pseudo-functions[6-11] fail to solve the problem because they are based on calculus performed taking into account only point saturation functions.

## Extension of the Methodology

In this work, an adequate methodology to adapt laboratory relative permeability curves to the curves needed for numerical simulation of linear system is presented. A similar type of transformation should be generalized for 2D systems.

The generalization to 3 dimensional systems is not needed because laboratory curves take into account only viscous forces. Without the presence of capillary or gravitational forces, the thickness of the system does not affect the advance frontal theory equations.

In order to take into account the third dimension it is desirable to maximize the vertical discretization by having a detailed vertical grid. This would allow the simulator to solve the problem taking capillarity and gravitational influences as a function of flow velocity.

## Conclusions

1. The relative permeability curve to be used in a material balance should relate the average saturation of the system with its ability to produce the fluids at the wells. In this way, the average relative permeability curves, taking into account the different forces acting at reservoir scale, should be used for that application. In absence of capillary or gravitational forces, the average curves here discussed must be used.

2. The proposed methodology of relative permeability upscaling honors the physics of a fluid flow dominated by viscous forces while it cancels out numerical dispersion.

3. The use of this kind of scaled-up relative permeability curves allows the reduction, when possible, of the number of horizontal gridcells in finite difference numerical simulations. In this way, a more detailed vertical layering could be included while keeping controlled the demand of computational resources.

4. Allowing a more detailed vertical discretization classical pseudo-functions are avoided. As a result, the simulator can solve viscous/capillar/gravitational equilibrium in a more effective way.

## Nomenclature

$A$ = Area, cm$^2$.
$k$ = Absolute permeability, darcys.
$kr_o$ = Oil relative permeability.
$kr_w$ = Water relative permeability.
$L$ = Length, cm.
$N$ = Original oil in place, m$^3$.
$Np$ = Cumulative oil produced. m$^3$.
$q_o$ = Oil rate, cm$^3$/s.
$q_w$ = Water rate, cm$^3$/s.
$Sw_{irr}$ = Irreducible water saturation, %.
$t$ = Time, seconds.
$V_o$ = Cumulative volume of oil produced, cm$^3$.
$V_t$ = Cumulative volume of total fluid produced, cm$^3$.
$\Delta P$ = Pressure difference, atm.
$\mu_o$ = Oil viscosity, cp.
$\mu_w$ = Water viscosity, cp.

## References

1. Jones, S.C., and Roszelle, W.O., "Graphical Techniques for Determining Relative Permeability from Displacement Experiments," J. Pet Tech. (May 1978), 807-817.
2. Buckley, S.E., and Leverett, M.C.: "Mechanism of Fluid Displacement in Sands," Trans. AIME (1942) **146**, 107-116.
3. Welge, H.J.: "A Simplified Method for Computing Oil Recovery by Gas or Water Drive," Trans. AIME (1952), **195**, 91.
4. Johnson, E.F., Bossler, D.P., and Naumann, V.O.: "Calculation of Relative Permeability from Displacement Experiments," Trans. AIME (1959) **216**, 370-372.
5. Dake, L.: "The Practice of Reservoir Engineering", Ed. Elsevier.
6. Coats, K.H., Dempsey, J.R. and Henderson, J.H.: "the Use of Vertical Equilibrium in Two Dimensional Simulation of Three Dimensional Reservoir Performance," *Soc. Pet. Eng. J.* (March 1971), 63-71.
7. Hearn, C.L.: "Simulation of Stratified Waterflooding by Pseudo Relative Permeability Curves," J. Pet. Tech. (July 1971), 805-813.
8. Jacks, H.H, Smith, O.J.E., and Mattax, C.C.: "The Modeling of a Three-Dimensional Reservoir With a Two-Dimensional Reservoir Simulator – The Use ofDynamic Pseudo Functions," *Soc. Pet. Eng. J.* (June 1973), 175-185.
9. Kyte, J.R., and Berry, D.W.: "New Pseudo-Functions to Control Numerical Dispersion," *SPE J.* 269 (1975).
10. Thomas, G.W.: "An Extension of Pseudofunction Concepts, paper SPE 12274, presented at the 1983 Reservoir Simulation Symposium, San Francisco, CA, 15-18 November.
11. Stone, H.L.: "Rigorous Black-Oil Pseudofunctions," paper SPE 21207, presented at the 1991 SPE Symposium on Reservoir Simulation, Anaheim, CA, 17-20 Februray.

**Tables**

| Table 1 - General Test Data | | |
|---|---|---|
| *Area* | 11.40 | cm$^2$ |
| *Length* | 12.71 | cm |
| *Poral Volume* | 31.14 | cm$^3$ |
| *$Sw_{irr}$* | 35.00 | % |
| *$k_o [Sw_{irr}]$* | 35.40 | MD |
| *$\mu_o$* | 10.50 | Cp |
| *$\mu_w$* | 0.97 | Cp |
| *$\Delta P$* | 100.00 | Psi |

| Table 2 - Displacement Test Results | | |
|---|---|---|
| *Time* Secs. | *$V_o$* cm$^3$ | *$V_t$* cm$^3$ |
| 0 | 0.00 | 0.00 |
| 180 | 3.09 | 3.09 |
| 372 | 7.00 | 7.00 |
| 540 | 7.80 | 10.90 |
| 720 | 8.33 | 15.28 |
| 900 | 8.70 | 19.89 |
| 1200 | 9.01 | 27.90 |
| 1560 | 9.32 | 37.80 |
| 3600 | 9.90 | 99.50 |
| 6000 | 10.09 | 176.80 |
| 9000 | 10.31 | 276.90 |

| Table 3 – Average Saturation Relative Permeability Curves | | |
|---|---|---|
| *Average Sw* % | *$Kr_o$* | *$Kr_w$* |
| 35.00 | | 0.000 |
| 44.92 | | 0.000 |
| 57.48 | 0.329 | 0.079 |
| 60.05 | 0.175 | 0.091 |
| 61.75 | 0.108 | 0.100 |
| 62.94 | 0.074 | 0.108 |
| 63.93 | 0.046 | 0.117 |
| 64.93 | 0.029 | 0.124 |
| 66.79 | 0.007 | 0.142 |
| 67.40 | 0.003 | 0.147 |
| 68.11 | 0.002 | 0.148 |

| Table 4 - Point Saturation Relative Permeability Curves[1] | | |
|---|---|---|
| *Average Sw* % | *$Kr_o$* | *$Kr_w$* |
| 35.00 | 0.774 | 0.000 |
| 51.10 | 0.285 | 0.065 |
| 53.40 | 0.200 | 0.076 |
| 58.00 | 0.087 | 0.095 |
| 61.70 | 0.030 | 0.106 |
| 64.60 | 0.010 | 0.124 |
| 66.40 | 0.003 | 0.136 |
| 67.60 | 0.002 | 0.145 |
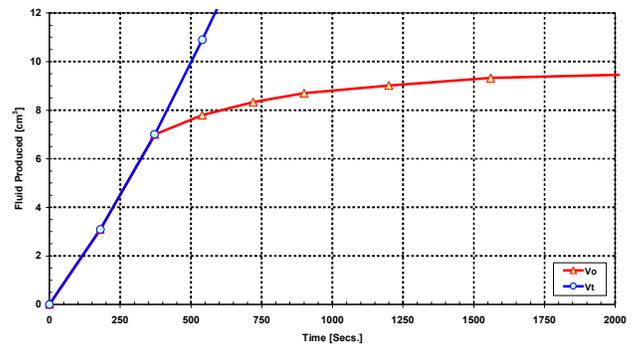
**Figures**



**Figure 1 – Production data of Jones & Roszelle experiment.**
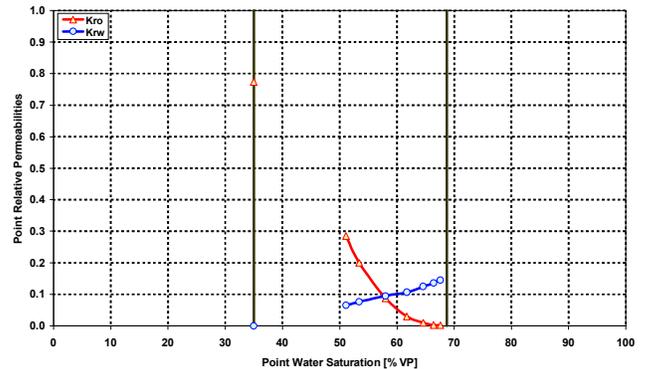


**Figure 2 – Point relative permeability curves.**
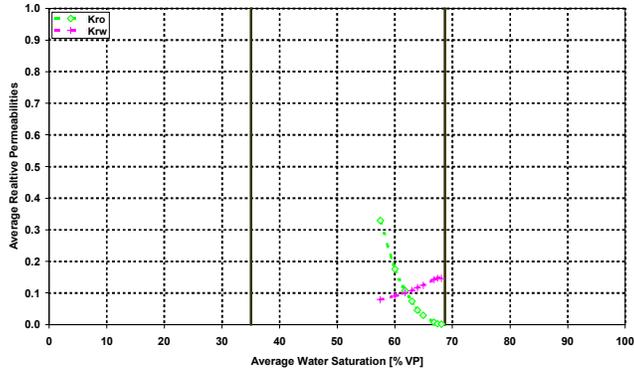
# Figures – cont.



**Figure 3 – Average relative permeability curves.**
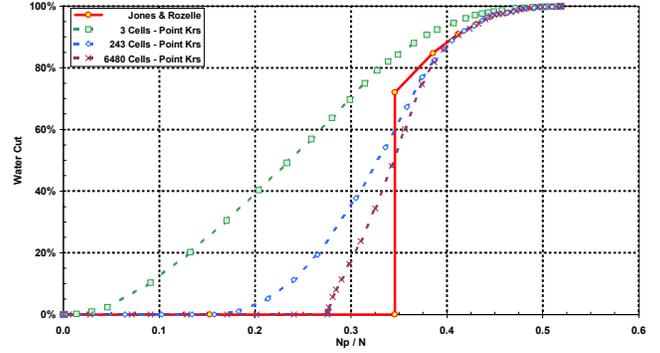


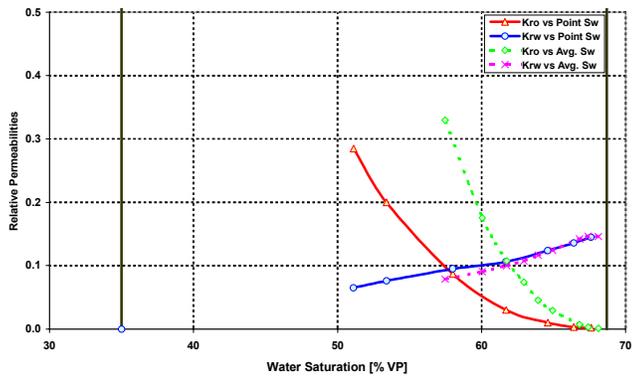**Figure 6 – Effect of number of gridcells on the results – point krs.**



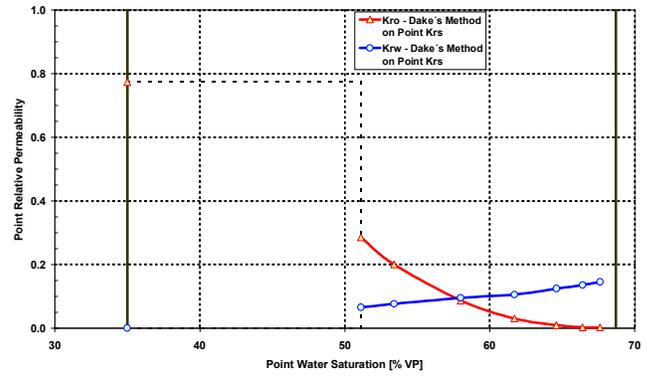**Figure 4 – Point vs. average relative permeability curves.**



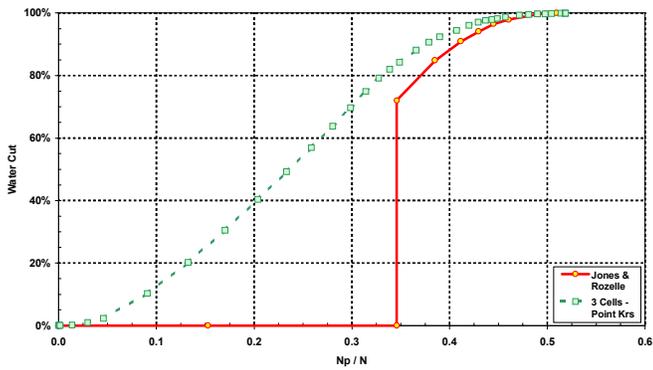**Figure 7 – Adapted point kr curves with Dake´s methodology.**



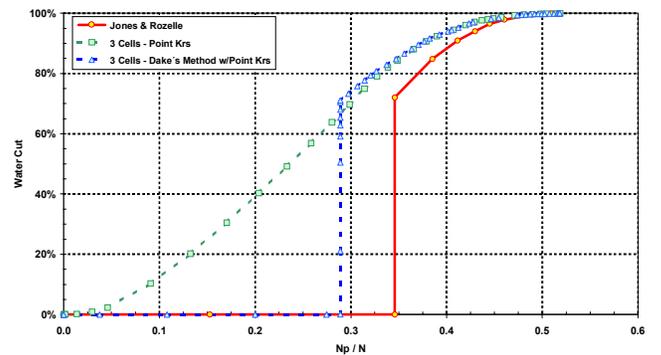**Figure 5 – Simulation results based on point krs vs. experimental.**



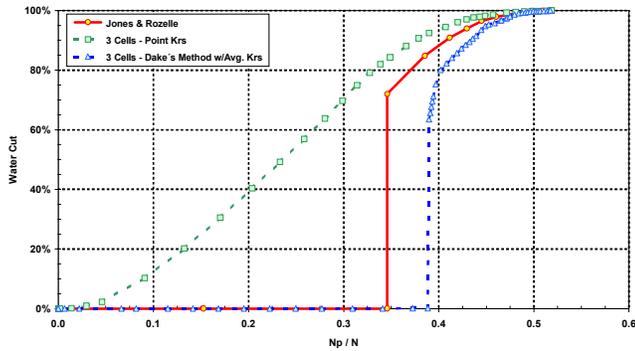**Figure 8 – Results using point krs with Dake´s modification.**

**Figures – cont.**



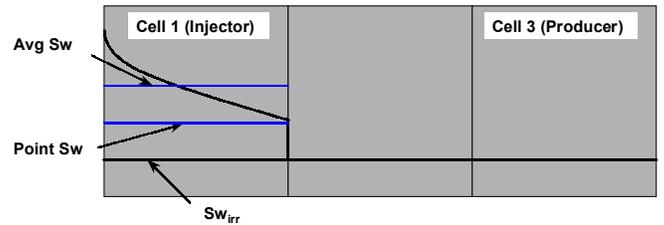**Figure 9 – Results using averaged krs with Dake´s modification.**



**Figure 12 – Point and average water saturation for cell 1.**



**Figure 10 – Mixing coeffs. of point and avg. krs (Combined Case).**
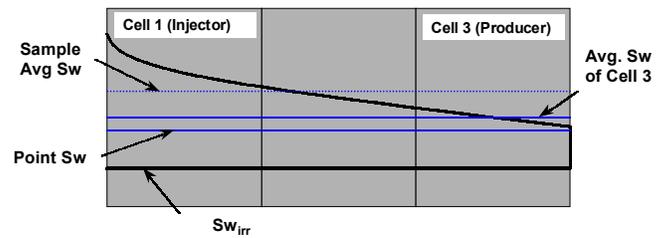
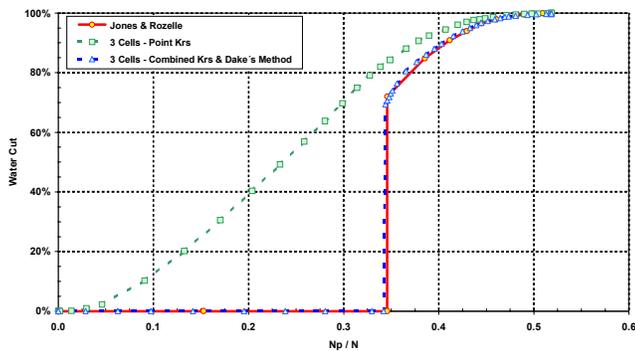

**Figure 13 – Point and average water saturation for cell 3.**



**Figure 11 – Results with "combined" krs & Dake´s methodology.**